Supporting Information

Attempts to realize promising thermoelectric performance in n-type polycrystal SnSe with cubic structure

Zhenqi Li[1], Yuping Wang[1], Dongrui Liu[1], Tao Hong[1*], Bingchao Qin[1,2,3*], Xiang Gao[4], Li-Dong Zhao[1,2,3*]

[1] *School of Materials Science and Engineering, Beihang University, Beijing 100191, China.*

[2] *Center for Bioinspired Science and Technology, Hangzhou International Innovation Institute, Beihang University, Hangzhou 311115, China.*

[3] *Tianmushan Laboratory, Beihang University, Hangzhou 311115, China.*

[4] *Center for High Pressure Science and Technology Advanced Research (HPSTAR), Beijing 100094, China.*

Corresponding authors:

*Email: hongtao77@buaa.edu.cn.

*Email: qinbingchao@buaa.edu.cn.

*Email: zhaolidong@buaa.edu.cn.

Experiment details

Sample synthesis: The high-purity elements of Sn, Se, Ag, Bi, Br, and Pb were weighed according to the stoichiometric ratio $(SnSe)_{1-x}(AgBiSe_2)_x$ (x = 0.3 and 0.4), $(SnSe_{1-y}Br_y)_{0.6}(AgBiSe_2)_{0.4}$ (y = 0.01, 0.03, and 0.05) and $(Sn_{1-z}Pb_zSe_{0.97}Br_{0.03})_{0.6}(AgBiSe_2)_{0.4}$ (z = 0, 0.05, 0.1, 0.15, 0.2, 0.3, and 0.4) and for reactive materials such as Br, they were weighed in a glove box protected by an N_2 atmosphere in the form of $SnBr_2$. The resulting mixture of target weights were loaded into quartz tubes pre-coated with a carbon layer, evacuated to below 10^{-4} Torr and flame sealed. All samples were synthesized by the melt method. The sealed quartz tubes were then placed in larger diameter outer quartz tubes and subjected to the same evacuation and flame sealing operation to prevent oxidation of the product due to rupture of the inner tubes as a result of the phase change during the cooling process. The tubes were loaded into a muffle furnace and slowly heated to 1223 K for 12 h, then kept for 12 h, cooled to 793 K for 6 h, kept for 12 h, and then slowly cooled to room temperature in the muffle furnace. The obtained ingots were ground into powder with agate mortar, passed through a 200-mesh sieve, and then subjected to spark plasma sintering (SPS-211Lx) on a graphite mold with a diameter of 15 mm under an axial compressive stress of 50 MPa for 5 minutes at a vacuum of 773 K. Dense cylindrical samples with a size of Φ15 × 8 mm^3 were finally obtained, and then they were cut and polished to further measurements.

X-ray diffraction: For the obtained samples, the phase structures were analyzed and characterized firstly. The ingots were manually ground to a powder and then passed

through a 200-mesh sieve used for phase analysis. The phase purity and identity were analyzed by the *D*/max 2500PC diffractometer equipped with Cu Kα (λ = 1.5418 Å) radiation.

Electrical transport properties: The samples were cut perpendicular to the pressure direction into rectangular samples of ~ 3 × 3 × 8 mm^3 for simultaneous measurement of electrical conductivity and Seebeck coefficient of the samples over the temperature range of room temperature to 773 K under helium atmosphere using an Advance Riko ZEM-3 instrument to calculate the power factor. The four-probe method was used, and the contact point between the sample and the probe was lined with carbon paper, which can effectively eliminate the influence of the contact resistance between the probe and the sample on the test results. The sample was coated with a thin layer of Boron Nitride (BN) to protect the instrument from possible damage caused by evaporation of the sample at high temperatures. The uncertainty of the Seebeck coefficient and conductivity measurements was within 5%.

Thermal transport properties: The obtained samples were cut and polished into 6 mm diameter discs with uniform thickness in the range of 1 mm to 2 mm for thermal diffusion coefficient (*D*) measurements. The *D* values from room temperature to 773 K were measured by laser flash method using a Netzsch LFA457 instrument made in Germany, and the thermal diffusion coefficient data were analyzed using a Cowan model with pulse correction. During the test, the top and bottom surfaces of the circular samples were coated with a thin layer of graphite to maximize the absorption of the

laser signal by the sample and minimize errors due to material emissivity. The thermal conductivity of the material was calculated according to the equation $\kappa = D \times \rho \times C_p$, where ρ is the density of the sample determined using the sample dimensions and mass and verified using the Archimedes test method, and C_p is the specific heat of the samples, which was generally taken to be calculated according to Dulong-Petitlaw in this work. Taking into account all uncertainties in D, ρ and C_p, the uncertainty in the total thermal conductivity was within 8%. Combining all the uncertainties in the testing process of the thermal and electrical transport parameters, the uncertainty in the ZT value was within 20%.

Microstructure characterization: The transmission electron microscopy (TEM) samples were first cut and polished until the sample thickness reaches 20-30 μm, followed by Ar-ion milling using a Precision Ion Polishing System Model 695 PIPSII (Gatan) with an applied voltage of 0.2-3.5 KV and a low temperature of 120 K. The microstructural analysis of the sample was mainly performed using the scanning transmission electron microscopy (STEM) mode conducted by a JEM-ARM200F (JEOL) microscope working at 200 KV.

Atomic-level energy spectrum acquisition methods: Achieving high-quality atomic-level energy spectrum images requires precise control over the stability of the imaging process. Environmental factors and electron irradiation can induce vibrations or drift in the sample, which significantly degrade the quality of atomic-level images. By effectively managing these issues, we enhance our chances of capturing exceptionally

clear atomic-level energy spectrum images. To mitigate carbon contamination on the sample surface, we conduct a pre-spectrum collection beam shower. This approach helps reduce contamination during imaging, but it's critical to complete the collection within one-hour post-shower to avoid renewed contamination. Moreover, due to inherent delays in sample movement, once the sample stops, it tends to drift in the direction it was last moved, requiring additional stabilization time to minimize this drift. Electron beam exposure on the sample can also alter images, leading to blur or drift. To facilitate atomic-level energy spectrum data acquisition, we must shorten the scanning time, allowing the electron beam to swiftly scan across the interface. However, beam blanking is impractical since electron beam interaction is essential for imaging. If the beam were not continuously active, the images taken before and after irradiation would differ significantly, complicating drift correction by software. Therefore, when acquiring atomic-level spectra, it's advisable to zoom directly to the desired magnification, observe the atomic vibrations and drift, and proceed once stability is achieved. Additionally, if the spectrum software permits, different filtering modes can be explored to find the most effective one. All these considerations play pivotal roles in enhancing the quality of atomic-level energy spectrum imaging.

Calculation details

The details for calculating the average ZT (ZT_{ave}) value is as follow:

$$ZT_{ave} = \frac{1}{T_h - T_c} \int_{T_c}^{T_h} ZT \, dT \quad (1)$$

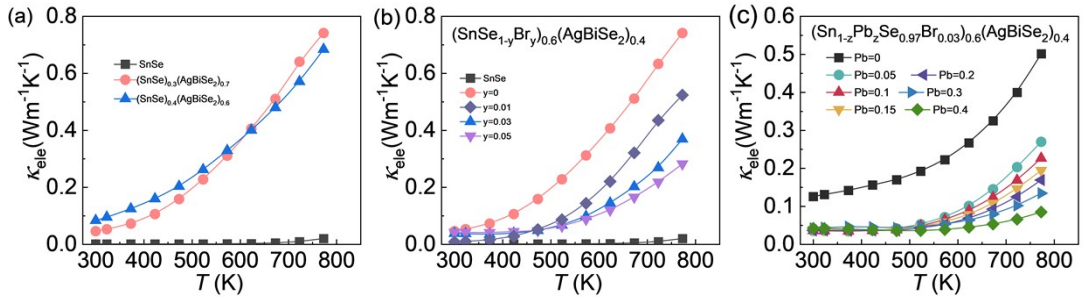

Figure S1. The electronic thermal conductivity of $(SnSe)_{1-x}(AgBiSe_2)_x$ samples (x = 0.3and 0.4), $(SnSe_{1-y}Br_y)_{0.6}(AgBiSe_2)_{0.4}$ samples (y = 0.01, 0.03, and 0.05), and $(Sn_{1-z}Pb_zSe_{0.97}Br_{0.03})_{0.6}(AgBiSe_2)_{0.4}$ samples (z = 0, 0.05, 0.1, 0.15, 0.2, 0.3, and 0.4).

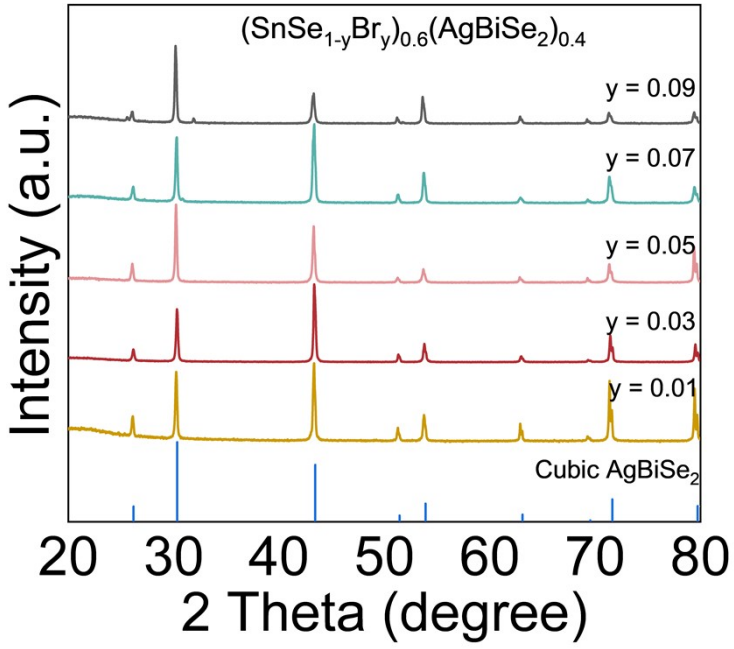

Figure S2. The powder X-ray diffraction (PXRD) patterns of $(SnSe_{1-y}Br_y)_{0.6}(AgBiSe_2)_{0.4}$ samples (y = 0.01, 0.03, 0.05, 0.07, and 0.09).

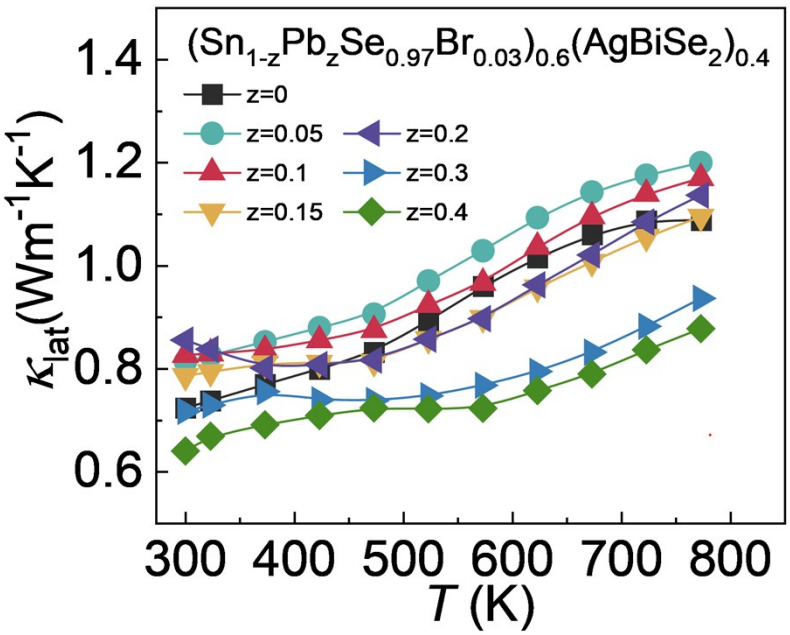

Figure S3. The lattice thermal conductivity of $(Sn_{1-z}Pb_zSe_{0.97}Br_{0.03})_{0.6}(AgBiSe_2)_{0.4}$ samples (z = 0, 0.05, 0.1, 0.15, 0.2, 0.3, and 0.4).